A TIME-RESOLVED SEM MONITOR WITH LARGE DYNAMIC RANGE*

M. Hori†, Max-Planck-Institut für Quantenoptik, Garching, Germany and
Department of Physics, University of Tokyo, Japan
K. Hanke, CERN, Geneva, Switzerland

Abstract

CERN's Linac4 will provide 160-MeV H^- beams of intensity $N = 2 \times 10^{14}$ ions s^{-1}. Before this beam can be injected into the existing CERN Proton Synchrotron Booster (PSB), a beam chopper must be used to remove some sequences of 0.5-ns-long micro-bunches from it. We developed a monitor to measure the time structure and spatial profile of the chopped beam, with respective resolutions $\Delta t \sim 1$ ns and $\Delta x \sim 2$ mm. Its large active area 40 mm × 40 mm and dynamic range also allows investigations of beam halos. The beam was first allowed to strike a carbon foil, and the resulting secondary electrons were accelerated by sets of parallel grid electrodes. The electrons then struck a phosphor screen, and the scintillation light was guided to a thermoelectrically cooled, charge-coupled device camera. The sub-nanosecond time resolution was attained by applying high-voltage pulses to the grids. The monitor has been tested with 700-ps-long UV laser pulses, and a 3-MeV proton beam provided by a tandem.

INTRODUCTION

In the planned design of Linac4 [1, 2, 3, 4], a H^- beam is accelerated to energy $E = 3$ MeV in a radiofrequency quadrupole (RFQ) which is excited at frequency $f_e = 352.2$ MHz. The beam emitted from the RFQ output thus consists of a train of 500-ps-long micro-bunches that each contain 10^9 ions and are spaced by intervals of $f_e^{-1} = 2.8$ ns. A beam chopper [1, 5] positioned downstream of the RFQ is planned to remove 133 consecutive micro-bunches out of every 352 in the beam. It is here crucial to remove all the ions in the bunches, as the ions would otherwise miss the longitudinal acceptance of the PSB, strike its inner walls, and radioactivate the accelerator. In this paper, we describe a monitor [6] which characterizes and validates the time evolution of the spatial profile of this chopped beam. More technical details can be found in Ref. [6].

* Work supported by European Community-Research Infrastructure Activity (CARE, RII3-CT-2003-506395), the Grant-in-Aid for Creative Basic Research (10NP0101) of Monbukagakusho, the European Young Investigator Awards (EURYI) of the European Science Foundation, and the Munich Advanced Photonics Cluster of the Deutsche Forschungsgemeinschaft (DFG).

† Masaki.Hori@cern.ch

MONITOR PRINCIPLE AND CONSTRUCTION

In this monitor, the H^- ions were first allowed to strike a carbon foil of thickness $t_d = 50\,\mu g \cdot cm^{-2}$ (Figure 1) which was placed at a 45-degree angle with respect to the H^- beam. The secondary electrons emitted from the foil were moved out of the path of the H^- beam and collected on a phosphor screen. The image of the scintillation light propagated along a fiber optic conduit, and was photographed by a charge-coupled device (CCD) camera. CCD's and phosphor screens are normally used as integration devices because of their slow (ms-scale) response times. In this monitor, however, a resolution $\Delta t \sim 1$ ns was attained by applying high voltage (HV) pulses of sub-nanosecond rise or fall times on a grid electrode and the phosphor screen, which controlled the flow of secondary electrons from the foil to the phosphor [7]. The monitor could be gated off during the strong H^- micro-bunches, and turned on within ~ 500 ps to verify whether there were any residual particles in the chopped bunches. The CCD normally had a dynamic range of ~10^4 against single micro-bunches of the beam. As we shall described below, this could be further increased by many orders of magnitude by exposing the CCD over several micro-bunches.

Initial acceleration of the electrons was provided by a grid [8] which was positioned parallel to the carbon foil at a distance $l \sim 7$ mm from it, and in the path of the H^- beam. The grid consisted of 25 graphite filaments of diameter $d = 5\,\mu$m (manufactured by Toray Industries K.K.). Calculations showed that the filaments would heat up ($T > 2000\,^\circ$C) and break, if the full RFQ beam intensity of $I = 70$ mA were focused into a 1-mm-diameter spot on their surface. The filaments would easily survive at d ~10 mm and reduced values of the duration Δt_m ~100 ns and repetition rate $f_r \leq 1$ Hz of the RFQ macro-pulses. We plan to validate the chopped beam at this reduced intensity, once the RFQ is constructed.

Next the electrons traversed a series of grids, including one with a specific structure which allowed 1-kV pulses of sub-nanosecond fall time to be applied to it. The grid surface of 50 mm × 50 mm was segmented into four 12.5 mm × 50 mm strips, parallel to the wires. The segments were connected to four gold striplines printed by thick-film methods on the ceramic frame. The widths and thicknesses of the segments were carefully adjusted to attain a characteristic impedance $Z_0 = 50\,\Omega$. The grid potential could thus be driven with an avalanche diode switch (Kentech Instruments HMP1/s/v), which simultaneously

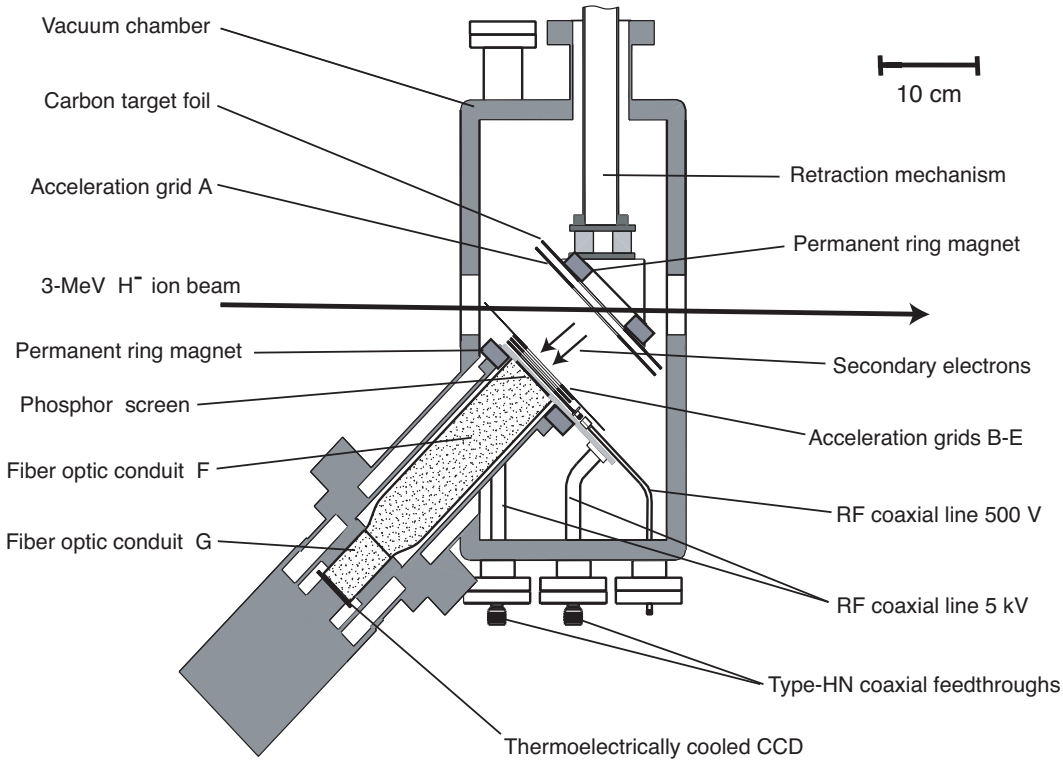

Figure 1: Schematic layout of the beam profile monitor. Incident H^- ions of energy $E = 3$ MeV struck a carbon target foil. Secondary electrons emitted from the foil were accelerated by grids A–E, and struck a phosphor screen. The fluorescence image was transported by fiber optic conduits F and G to a CCD.

generated HV pulses of amplitude $V = -500$ V and fall time $t_r \sim 200$ ps on the four lines without impedance mismatch.

The phosphor screen was manufactured by first depositing a layer of indium tin oxide on the surface of a 50 mm × 50 mm fiber optic plate. The plate consisted of 6-μm-diameter optical fibers which were bundled together. A layer of 1-μm-diameter grains of gadolinium oxysulphide doped with terbium (Gd_2O_2S : Tb, P43), followed by a 40-nm-thick aluminium layer was deposited on the plate. The aluminium layer served three purposes, i): only electrons accelerated to energy $E > 3$ keV could penetrate the layer and produce scintillation light, whereas lower-energy electrons were stopped by it. The detector could thus be quickly turned on or off by adjusting the incident energy of the secondary electrons, ii): it prevented stray light, or the glow from the carbon foil heated by the H^- beam, from entering the fiber optic bundle and producing spurious images, iii): it increased the collection efficiency of the fluorescence light from the screen.

The screen was mounted on a ceramic frame, and four gold striplines of impedance $Z_0 = 50\,\Omega$ were printed on the ceramic and connected to the aluminium surface of the screen. This allowed a voltage pulse of amplitude 6–7 kV and rise-time $t_r \sim 500$ ps to be applied on the phosphor screen, by driving the four lines simultaneously using another switch (Kentech Instruments PBG3/s/v). The pulses propagated along four parallel coaxial cables of length $l = 2$ m, and arrived simultaneously at the phosphor screen. As the screen presented an open circuit at the end of the coaxial lines, it reflected the voltage pulses, which then returned to the switch. At the position of the phosphor screen, the leading edge of the reflected pulse overlapped with the counterpropagating trailing edge [9], and this collision caused the potential on the phosphor screen to double its amplitude, to $V \sim 6$ kV needed for the gating.

MEASUREMENTS WITH UV LASER BEAM

We generated UV laser pulses of energy $E \sim 5$ mJ, wavelength $\lambda = 266$ nm, and pulse length $\Delta t \sim 700$ ps to simulate the time structure of the micro-bunches expected in Linac4. This was accomplished by using a stimulated Brillouin scattering (SBS) cell [6, 10, 11] to temporally compress the output of a Q-switch Nd:YAG laser. We replaced the carbon target foil with a gold photocathode foil, and irradiated it with the UV laser beam of energy $E = 10$–200 μJ to generate $N_\gamma = 2 \times 10^7 - 4 \times 10^8$ photoelectrons per incident laser pulse. This simulated the monitor response against the secondary electrons produced by the Linac4 beam.

In Fig. 2 (a)–(f), the spatial profiles corresponding to the time profiles between $t = -2$ ns and 3 ns are shown. These

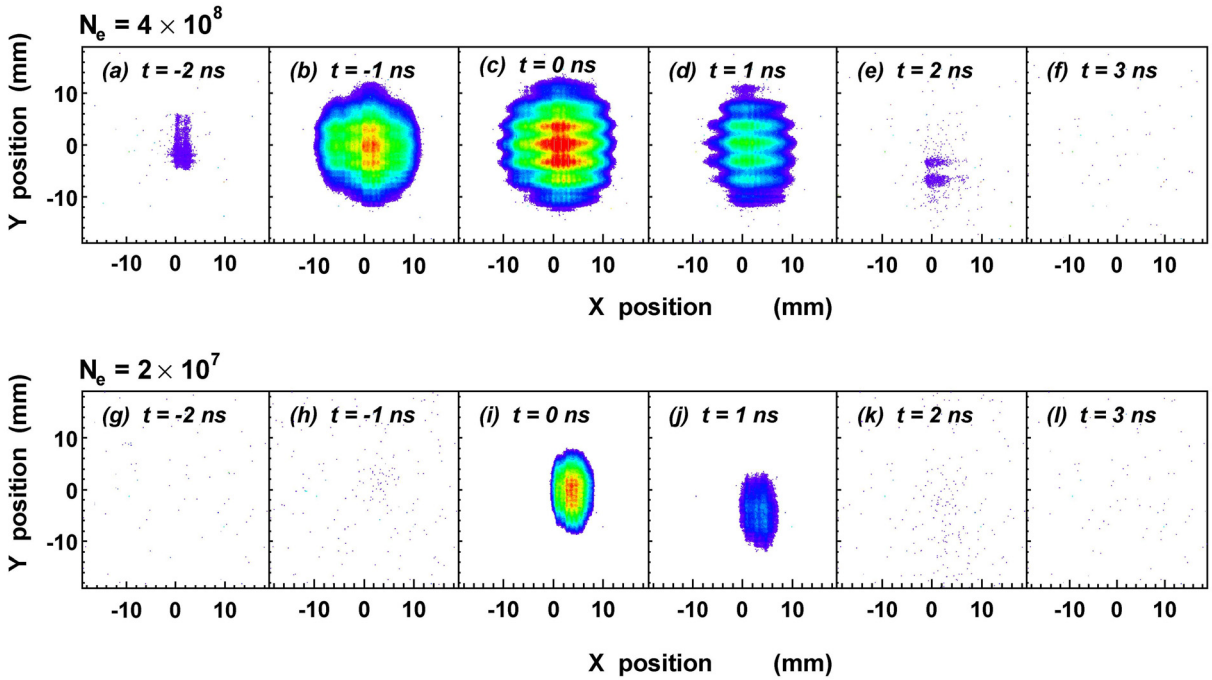

Figure 2: Sequence of CCD exposures taken of the UV laser pulses which simulate the expected intensities of the Linac4 beam . Profiles (a)–(f) were measured at a photoelectron intensity $N_e = 4 \times 10^8$, whereas (g)–(l) were measured at $N_e = 2 \times 10^7$.

are analogous to stop-motion photographs of the beam with a 1-ns-scale resolution. Although the laser beam on the photocathode was adjusted to vertical and horizontal diameters $d_v \sim 8$ mm and $d_h \sim 3$ mm, the CCD images were much larger ($d \sim 15$ mm). This blow-up is due to space-charge effects in the photoelectron beam during transport from the photocathode to the phosphor screen. Several vertical and horizontal bands are seen in Fig. 2 (c)–(d), which were presumably caused by the deflection of the photoelectron trajectories near the grid filaments during the above blow-up. The photoelectrons were multiplied when they struck the acceleration grids, and this could also contribute to this band structure.

To avoid these space-charge effects, we used a lower intensity in the UV laser. This corresponds to a much lower number $N_e = 2 \times 10^7$ of photoelectrons emitted from the photocathode per laser pulse. The spatial profiles measured at these conditions are shown in Fig. 2 (g)–(k). The band structure and blow-up have now been reduced. The relative amplitude of the spurious afterpulses are much smaller (typically ~0.5% of the main pulse).

MEASUREMENTS WITH PROTON BEAM

We carried out an experiment using the Tandem facility of the Institut de Physique Nucléaire, Orsay, to study the response of the monitor against a 3-MeV proton beam. This facility provided 5-ns-long micro-bunches containing $N_p = 5 \times 10^4$ protons, which arrived with a repetition rate $f = 10$ MHz. The spatial resolution for cases wherein the secondary electrons were accelerated between the foil and phosphor with an energy $E = 8$ keV was $\Delta x < 2$ mm. Space-charge effects at the low beam intensities induced negligible blow-up in the CCD image, which is in good agreement with the results of particle-tracking simulations.

We studied the dynamic range and sensitivity of the monitor, by measuring its response against a 10-mm-diameter proton beam of various intensities, between $N_p =$ 10 and 6×10^4 protons per micro-bunch. Figure 4 shows the integrated signal on the CCD, as a function of the number of protons arriving at the foil as calibrated using a Faraday cup. A linear response was observed over the four orders of magnitude in beam intensity that was accessible by the tandem, within the systematic error of the Faraday cup readings. Clear signals were observed at the lowest proton intensities $N_p \sim 10$. In conclusion, this monitor is now adequate to validate the chopped beam of the Linac4 RFQ at the intensities and time structures expected for PSB injection. The device must however be further improved if it is to be used in future facilities with even higher beam intensities. The largest problem when using this monitor was the space-charge effect [12] at high currents of the secondary electrons, and the high amplitudes of spurious prepulses and afterpulses that this induces. One possibility for reducing these spurious pulses may be to add more switching electrodes to the monitor. We had previously studied the afterpulses that occur in gated photomultipliers [7]. By switching the potentials of the photocathode and four dynodes simultaneously, we suppressed the intensity of the afterpulses to 5×10^{-4} relative to the main pulse. How-

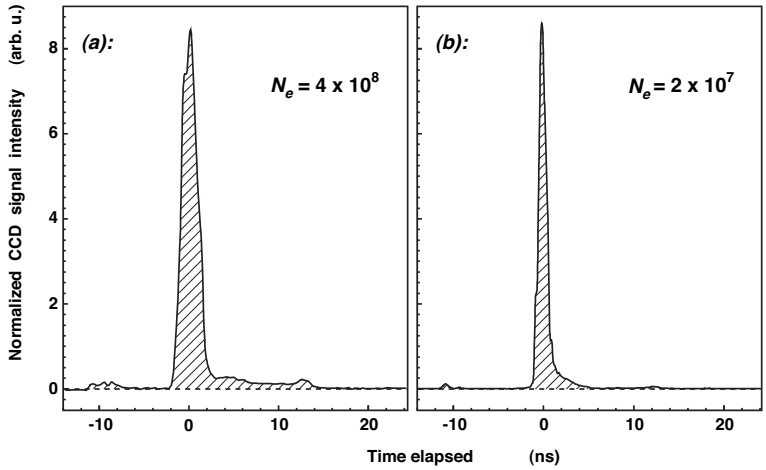

Figure 3: Time profile of the UV laser pulse measured by the monitor, at an intensity corresponding to $N_e = 4 \times 10^8$ (a) and $N_e = 2 \times 10^7$ (b) photoelectrons. Note that the signal intensity of (a) is greater than that of (b) by an order of magnitude, whereas we here plot the normalized intensities.

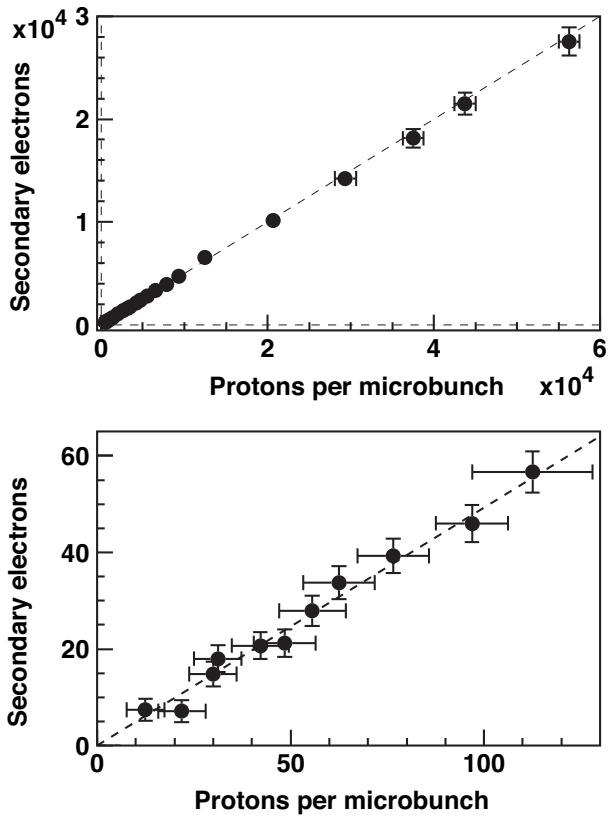

Figure 4: Intensity of the CCD signals, as a function of the number of 3-MeV protons in each 5-ns-long micro-bunch arriving at the carbon foil. The measurements were made by integrating the signals from 10^3 micro-bunches on the CCD.

ever, since residual gases in the accelerator vacuum may be ionized by the signal electrons, it may be difficult to completely suppress the spurious pulses below a relative intensity of 10^{-4} using electrodes alone. An alternative way of eliminating these effects may be to use the laser described here to photoionize the H^- beam, instead of intercepting the beam with a target foil or filament. This would result in a smaller number of signal electrons reaching the phosphor screen.

REFERENCES

[1] L. Arnaudon et al., Linac4 technical design report, CERN-AB-2006-084 ABP/RF, CERN, Geneva, 2006.

[2] C. Rossi et al., "The SPL front end: A 3 MeV H^- test stand at CERN", Proceedings of LINAC 2004, Lübeck, Germany, 2004.

[3] M. Vretenar et al., "Linear accelerator designs for the upgrade of the CERN proton injector complex (Linac4, SPL)", Proceedings of the Asian particle accelerator conference 2007, Indore, India, 2007.

[4] F. Gerigk et al., Conceptual design of the SPL II - A high-power superconducting H^- linac at CERN, CERN-2006-006, CERN, Geneva, 2006.

[5] T. Kroyer, F. Caspers, E. Mahner, "The CERN SPL chopper structure - A status report", CARE-report-2006-033-HIPPI, CERN, Geneva, 2007.

[6] M. Hori, K. Hanke, Nucl. Instr. and Meth. A 588 (2008) 359.

[7] M. Hori, K. Yamashita, R.S. Hayano, T. Yamazaki, Nucl. Instr. and Meth. A 496 (2003) 102.

[8] M. Hori, Rev. Sci. Instrum. 76 (2005) 113303.

[9] M.J. Eckart, R.L. Hanks, J.D. Kilkenny, R. Pasha, J.D. Wiedwald, J.D. Hares, Rev. Sci. Instrum. 57 (1986)

[10] D. Neshev, I. Velchev, W.A. Majewski, W. Hogervorst, W. Ubachs, Appl. Phys. B 68 (1999) 671.2046.

[11] M. Hori, R.S. Hayano, M. Fukuta, T. Koyama, H. Nobusue, J. Tanaka, Rev. Sci. Instrum. 80 (2009) 103104.

[12] M. Hori, Nucl. Instr. and Meth. A 522 (2004) 420.